The Astronomical Journal, 156:220 (12pp), 2018 November https://doi.org/10.3847/1538-3881/aae3ea

Photometric and Spectroscopic Studies of Four New Low-mass M-type Eclipsing Binaries

Liu Long[1,2], Li-Yun Zhang[1,2,5], Xianming L. Han[1,2,3], Hong-Peng Lu[1,2], Qing-feng Pi[4], and Qiang Yue[1,2]
[1] College of Physics/Department of Physics and Astronomy & Guizhou Provincial Key Laboratory of Public Big Data, Guizhou University, Guiyang 550025, People's Republic of China; liy_zhang@hotmail.com
[2] Key Laboratory for the Structure and Evolution of Celestial Objects, Chinese Academy of Sciences, Kunming 650011, People's Republic of China
[3] Dept. of Physics and Astronomy and SARA, Butler University, Indianapolis, IN 46208, USA
[4] Department of Astronomy, Beijing Normal University, Beijing, 100875, People's Republic of China
Received 2018 July 24; revised 2018 September 15; accepted 2018 September 18; published 2018 October 25

Abstract

We performed multicolor photometric and spectroscopic observations of four new low-mass M-type eclipsing binaries (HAT 225-03429, CRTS J085623.0+282620, CRTS J110302.4+201611, 2MASS J16344899+3716423) in 2017. We obtained new *VRI* light curves and minimum times of these four systems. Based on our minimum times, we updated the orbital periods and the linear ephemerides using the least squares method. We analyzed these four systems using the Wilson–Devinney program, and obtained the orbital and starspot parameters. The results of our analysis of the light curves indicate that HAT 225-03429 and CRTS J085623.0+282620 are detached eclipsing binaries, CRTS J110302.4+201611 is a semi-detached eclipsing binary, and 2MASS J16344899+3716423 is a contact binary. We performed LAMOST spectroscopic studies of chromospheric activity indicators (H_α, H_β, H_γ, H_δ, and Ca II H&K lines) for these four systems for the first time. We first determined their spectral types and calculated the equivalent widths of their chromospheric active indicators. These indicators show that the four low-mass M-type eclipsing binaries are active. Furthermore, the radii of these stars are notably larger than model predictions for their masses, except for the secondary component of HAT 225-03429 and the primary component of CRTS J110302.4+201611.

Key words: binaries: eclipsing – starspots – stars: individual (HAT 225-03429, individual CRTS J085623.0 +282620, CRTS J110302.4+201611, 2MASS J163)

Supporting material: machine-readable table

1. Introduction

Low-mass stars are defined as $M < 0.8\,M_\odot$. They are the most common type of stars in the Galaxy (Kroupa et al. 2013), yet they remain elusive and mysterious objects. Because of their mass being lower than the Sun's, they also have cool surface temperatures and very low intrinsic brightness. In spite of so many obstacles, low-mass stars have been discovered one after the another. Low-mass stars usually have high levels of magnetic activities. In many cases, magnetic activities manifest themselves in the form of starspots, flares, and plages (e.g., Plibulla et al. 2003; Berdyugina 2005; Strassmeier 2009; Zhang et al. 2017). Chabrier et al. (2007) put forward the hypothesis that observed temperature and radius differences were results of convection caused by rotation and/or the magnetic field, as well as the existence of large surface magnetic spots. The magnetism of these stars may influence their structure and evolution in a variety of ways (Browning et al. 2016).

Present evolutionary models for stars with mass in the range of 0.4–0.8 $M_\odot$ predicts ∼5%–15% smaller radii and ∼3%–5% higher effective temperatures than the observed values (e.g., Baraffe et al. 1998; Ribas 2006; Coughlin et al. 2011). These differences between observations and models of low-mass stars have been discussed by several authors (e.g., Baraffe et al. 1998; Morales et al. 2010). Therefore, it is of great significance to study the formation of low-mass stars and compare their parameters with those predicted by theoretical stellar models. To better understand the magnetic activities of low-mass M-type eclipsing binaries, multicolor photometric and spectroscopic observations are necessary.

The majority of stars in our Galaxy are M dwarfs, making up about two-thirds of the population and about forty percent of stellar mass (Kirkpatrick et al. 2012). In spite of this, very few M dwarf eclipsing binaries were known because most M dwarfs are very faint at optical bands. Although M dwarfs have been somewhat overlooked in the past, for the above reason, more and more M dwarfs have gradually been discovered in recent surveys, such as the Sloan Digital Sky Survey (SDSS; York et al. 2000; Hawley et al. 2002; Raymond et al. 2003; Deshpande et al. 2013; Pineda et al. 2013), Pan-STARRS1 Medium Deep Survey (PS1-MDS; Kado-Fong et al. 2016), Two Micron All Sky Survey (2MASS; Skrutskie et al. 2006), Large Sky Area Multi-Object fiber Spectroscopic Telescope (LAMOST; Cui et al. 2012; Luo et al. 2015; Zhang et al. 2016, 2018), Deep Near-Infrared Southern Sky Survey (DENIS; Epchtein et al. 1999), and Catalina Sky Survey (CSS; Drake et al. 2014). West et al. (2004a, 2011) published a spectroscopic catalog of 70841 M dwarf from the seventh major data release of SDSS, and measured their spectral types and chromospheric properties. Later, Bochanski et al. (2011) provided a statistical parallax analysis using the catalog of low-mass M dwarfs. Using the Hα line, they also determined the magnetic activity fraction as a function of spectra type and their spatial dependence on M dwarf magnetic activity (e.g., West et al. 2011; Pineda et al. 2013). Recently, LAMOST also published about a catalog of about 100,000 M dwarfs (including spectral type, the equivalent width of Hα line, and radial velocity) and updated the relationship between the fraction of active stars and spectra types (e.g., Yi et al. 2014; Zhang et al. 2016, 2018). They also studied the chromospheric activity variation on short and long timescales (Zhang et al. 2016, 2018). West et al. (2015) also investigated the relationship between magnetic activity and rotation of

[5] Author to whom any correspondence should be addressed.

Table 1
Basic Properties for Four Low-mass M-type Eclipsing Binaries

Star Name	CSS_ID	R.A.(2000)	Decl.(2000)	V_{CSS}	P_F	A_V	Type
HAT 225-03429	CSS_J092128.3+332558	09 21 28.32	+33 25 58.4	14.06	0.42647	0.24	Algol-type (detached)
CRTS J085623.0+282620	CSS_J085623.0+282620	08 56 23.00	+28 26 20.5	14.36	0.354861	0.20	W UMa-type (contact)
CRTS J110302.4+201611	CSS_J110302.4+201611	11 03 02.45	+20 16 11.2	14.72	0.286646	0.10	W UMa-type (contact)
2MASS J16344899+3716423	CSS_J163448.9+371642	16 34 48.94	+37 16 42.4	14.27	0.246723	0.21	W UMa-type (contact)

Notes. Column 2: CSS_ID. Columns 3 and 4: R.A. and decl. (J2000). Column 5: average magnitude from AFD. Column 6: period in days. Column 7: amplitude from AFD. Column 8: types of periodic variables.

M stars. From PS1-MDS, Kado-Fong et al. (2016) discovered 270 rotating M dwarf candidates from 184,148 cool stars, and determined their masses, distances, temperature, and activities. Clark et al. (2012) used the spectra of 39,543 M dwarfs from the SDSS to measure the occurrence rate of binaries in M dwarfs. In addition, M dwarfs are currently considered to be the main targets for finding Earth-like exoplanets (Martín et al. 2005; Nutzman & Charbonneau 2008), due to their small star size leading to deeper transits and their smaller star mass resulting in larger reflex motion caused by planetary companions (Nefs et al. 2013). The low metal content and cool temperatures of M dwarfs provide favorable conditions for studying the formation of dust and clouds and their radiation transmission in the atmosphere (Rajpurohit et al. 2018).

Although most stars in the Galaxy are M dwarfs, our understanding of the relationship between temperature, metallicity, mass, and radius is still not prefect. One type of natural astrophysical laboratory for calibrating relationships between fundamental properties for low-mass stars is the M dwarf eclipsing binary (Torres & Ribas 2002; Ribas 2003; López-Morales & Ribas 2005; Morales et al. 2009a; Nefs et al. 2013; Zhang et al. 2014; Lubin et al. 2017). Previous researchers have precisely determined the stellar orbital parameters of M eclipsing binaries, as well as magnetic activities, such as starspots, flare events, and so on (e.g., Nefs et al. 2013; Zhang et al. 2014; Butler et al. 2015; Cruz et al. 2018). However, only a few M dwarf eclipsing binaries are currently known and have been characterized with appropriate accuracy to calibrate low-mass stellar evolution models, due to the intrinsic faintness of M dwarfs. Thus, it is necessary to further research M dwarf eclipsing binaries. While static all-sky surveys were able to reach object as faint as M dwarfs, the time-domain surveys were not deep enough; even the Catalina Real-Time Transient Survey (CRTS; Drake et al. 2009) and/or Palomar Transient Factory (Law et al. 2009; Rau et al. 2009) can only grasp early-type M dwarfs, let alone identify M dwarf eclipsing binaries of late M type. However, as the number of M dwarfs has increased, the study of a multiplicity of M dwarfs has gradually emerged. In addition, there are many M dwarf eclipsing binaries discovered as byproducts of transit exoplanet surveys, such as MEarth (Irwin et al. 2011, 2010, 2009) and the WFCAM Transit Survey (Birkby et al. 2012; Nefs et al. 2012, 2013; Cruz et al. 2018). The four M-type eclipsing binaries in this study (HAT 225-03429, CRTS J085623.0+282620, CRTS J110302.4+201611, and 2MASS J16344899+3716423) were discovered from the Catalina Sky Survey. The Catalina Sky Survey, which began in 2004, covers the sky with three telescopes at a decl. between $-75°$ and $+65°$ to find potential hazardous asteroids and near-Earth objects. Table 1 list some of the basic properties for these four eclipsing binaries from the Catalina Sky Survey.

HAT 225-03429 has been categorized as an Algol-type eclipsing binary with a period of 0.42647 day (Drake et al. 2014). Lee & Lin (2017) determined the masses and radii of HAT 225-03429 component stars with both radial velocity and light curves by the JKTEBOP (Southworth et al. 2004). They gave the absolute parameters of HAT 225-03429: $M_1 = 0.418\,M_\odot$, $M_2 = 0.300\,M_\odot$, $R_1 = 0.663\,R_\odot$, $R_2 = 0.478\,R_\odot$. They also gave other parameters of HAT 225-03429: the inclination angle $i = 73\overset{\circ}{.}5$, the separation of the two components $a = 2.148\,R_\odot$, and six radial velocities at phase 0.25. CRTS J085623.0+282620, CRTS J110302.4+201611, and 2MASS J16344899+3716423 have been classified as W Uma type, with periods of 0.354861, 0.286646, and 0.246723 days, respectively (Drake et al. 2014). No orbital parameters for CRTS J085623.0+282620, CRTS J110302.4+201611, or 2MASS J16344899+3716423 have been reported yet.

LAMOST spectral survey provides a rich database for studying spectroscopic properties of eclipsing binaries (Zhang et al. 2018). In this paper, we will present six new *CCD* light curves for these four systems obtained in 2017. We will also present our analyses of their chromospheric emissions using several corresponding LAMOST spectra.

2. Observations

In this work, we observed three of the four low-mass eclipsing binaries in 2017 (HAT 225-03429: 2017 February 26, 28, and March 2; CRTS J085623.0+282620: 2017 February 27, and March 1; CRTS J110302.4+201611: 2017 March 2.) using the 85 cm reflecting telescope at the Xinglong station of the National Astronomical Observatories of China (NAOC), which is equipped with a 1024×1024 pixel CCD (Zhou et al. 2009). We used the *VRI*, *RI*, and *VRI* filters for HAT 225-03429, CRTS J085623.0+282620 and, CRTS J110302.4+201611. We observed 2MASS J16344899+3716423 using the SARA 91.4 cm telescope at the Kitt Peak National Observatory (SARA KP) in Arizona on 2017 May 24 and June 11, and the Holcomb telescope in Indiana on 2017 May 17 and 22. The Holcomb telescope is a 94 cm Cassegrain Reflecting telescope with a focal ratio of $f/6.1$. It is equipped with a 2048×2064 CCD. The CCD camera of the SARA KP telescope has a resolution of 2048×2048 pixels, but we used it in 2×2 binning mode, leading to an effective resolution of 1024×1024. We used Bessel *VRI* and *RI* filters for the Holcomb telescope and the SARA KP telescope (Keel et al. 2017), respectively. The data observed by the Holcomb telescope is worse than that from the SARA KP telescope. We revised these data according to the magnitude differences of the different telescopes (the magnitude of the reference minus that of check stars). We listed the observation details in Table 2, which includes our objects, comparison stars, check stars, exposure times, and telescopes. The images are processed in

Table 2
Observation Log

Star Name	Comparison Star	Check Star	Exposure Time (Bands)	Telescope
HAT 225-03429	LEDA 2032278	TYC 2496-1338-1	110s, 45 s, 20 s (*VRI*)	85 cm
CRTS J085623.0+282620	2MASS J08563350+2825172	2MASS J08555812+2829135	45 s, 45 s (*RI*)	85 cm
CRTS J110302.4+201611	2MASS J11025409+2015583	2MASS J11030766+2016186	110 s, 50 s, 30 s (*VRI*)	85 cm
2MASS J16344899+3716423	2MASS J16344721+3713036	2MASS J16343067+3716200	90 s, 60 s, 60 s (*VRI*)	Holcomb, SASA KP

the standard method, which includes image trimming, bias and flat correction, cosmic ray removal, and aperture photometry. We plot the light curves of these systems in Figure 1. We listed the heliocentric Julian dates (HJD) and the magnitude differences in Table 3.

The spectroscopic observations for the four eclipsing binaries were made by LAMOST. We downloaded the spectroscopic data from the LAMOST website (http://dr5.lamost.org) (Luo et al. 2012; Zhao et al. 2012). We plotted these new spectra in Figure 2 to aid our systematic analyses of these four eclipsing binaries. We used Hammer program (West et al. 2004b) to determine their spectral types and found that our objects are M-type low-mass eclipsing binaries, and marked their spectral types in Figure 2.

3. Period Study

Based on our photometric data, we separately derived new minimum times for the four low-mass M-type eclipsing binaries using the program developed by Kwee & van Woerden (1965) and Nelson (2007). We listed our new minimum times and the corresponding errors for each filter of these four eclipsing binaries in Table 4. We also calculated the average minimum times and the corresponding errors and listed them in this table. Using the least squares method to fit the corresponding minimum times, we obtained updated linear ephemerides for these four eclipsing binaries as follows. The new linear ephemeris for HAT 225-03429 is:

$$\begin{aligned}\mathrm{Min.I} = {} & \mathrm{HJD}\ 2457811.1473(\pm 0.0070) \\ & + 0.43570740^{\mathrm{d}}(\pm 0.0000002)\mathrm{E}; \end{aligned} \quad (1)$$

for CRTS J085623.0+282620, it is:

$$\begin{aligned}\mathrm{Min.I} = {} & \mathrm{HJD}\ 2457812.0753(\pm 0.0005) \\ & + 0.35510675^{\mathrm{d}}(\pm 0.0000002)\mathrm{E}; \end{aligned} \quad (2)$$

for CRTS J110302.4+201611, it is:

$$\begin{aligned}\mathrm{Min.I} = {} & \mathrm{HJD}\ 2457815.1967(\pm 0.0007) \\ & + 0.28706666^{\mathrm{d}}(\pm 0.0000002)\mathrm{E}; \end{aligned} \quad (3)$$

and for 2MASS J16344899+3716423, it is:

$$\begin{aligned}\mathrm{Min.I} = {} & \mathrm{HJD}\ 2457897.8043(\pm 0.0010) \\ & + 0.24671940^{\mathrm{d}}(\pm 0.0000003)\mathrm{E}. \end{aligned} \quad (4)$$

E in the above equations is the epoch number. These binaries have only been discovered recently, so we do not yet have minimum times over long periods of time. As a result, we do not have sufficient data to analyze their period variations. Additional long-term observations are thus important for studying these eclipsing binaries.

4. Light Curve Analysis

In this section, we will analyze the orbital and starspot parameters, as well as the chromospheric activities of these four low-mass M-type eclipsing binaries.

4.1. The Orbital Parameter Analysis

Because our photometric data have high time resolutions and complete phase coverage, we can find the orbital solutions for these four low-mass M-type eclipsing binaries using the updated version of the Wilson–Devinney (WD) program, which is implemented in the FORTRAN programming language (Wilson & Devinney 1971; Wilson 1990, 1994; Wilson & Van Hamme 2004).

During this process, we set the fixed parameters in the WD program as follows: the gravity-darkening exponents were chosen as $g_1 = g_2 = 0.32$ (Lucy 1967) and the bolometric albedo $A_1 = A_2 = 0.5$ (Rucinski 1969). The limb-darkening coefficients and the bolometric limb-darkening coefficients were computed via the linear darkening law from Van Hamme (1993). The primary temperatures (T_1) were derived via the following formula (Collier Cameron et al. 2007):

$$T_{\mathrm{eff}} = -4369.5(J - H) + 7188.2,\ 4000\ \mathrm{K} < T_{\mathrm{eff}} < 7000\ \mathrm{K}. \quad (5)$$

In this equation, the values of J and K magnitudes can be obtained through the 2MASS All-Sky Catalog (Skrutskie et al. 2006). Using this equation, we determined the effective temperatures of the primary components for the four eclipsing binaries under this study and listed them in Table 5. These temperature values are consistent with their spectra.

HAT 225-03429 is an EA binary (Drake et al. 2014), so we used mode 2 (detached mode) to analyze its light curves. CRTS J085623.0+282620, CRTS J110302.4+201611, and 2MASS J16344899+3716423 have been classified as being W Uma type (Drake et al. 2014), so we used mode 3 (contact mode) to analyze their light curves. However, although we obtained converged solutions with mode 3 for CRTS J085623.0 +282620 and CRTS J110302.4+201611, their dimensionless potentials are larger than the Ω_{in}. Hence, it did not fit the physical norm for the contact model. Therefore, we tried to get appropriate solutions using other modes. Eventually, we obtained converged results with mode 2 for CRTS J085623.0 +282620 and mode 5 (semidetached with the secondary completely filling its limiting Roche bole) for CRTS J110302.4 +201611. It should be mentioned that there is no spectroscopic mass ratio for our targets (CRTS J085623.0+282620, CRTS J110302.4+201611, and 2MASS J16344899+3716423). As a result, we needed to search for the best mass ratio q (the ratio of M_2/M_1) that produces the least amount of fitting residuals. We plotted the fitting residual Σ versus q relationships in Figure 3. The lowest residuals occur at the mass ratio $q = 0.8$ for CRTS J085623.0+282620, 0.6 for CRTS J110302.4+201611, and

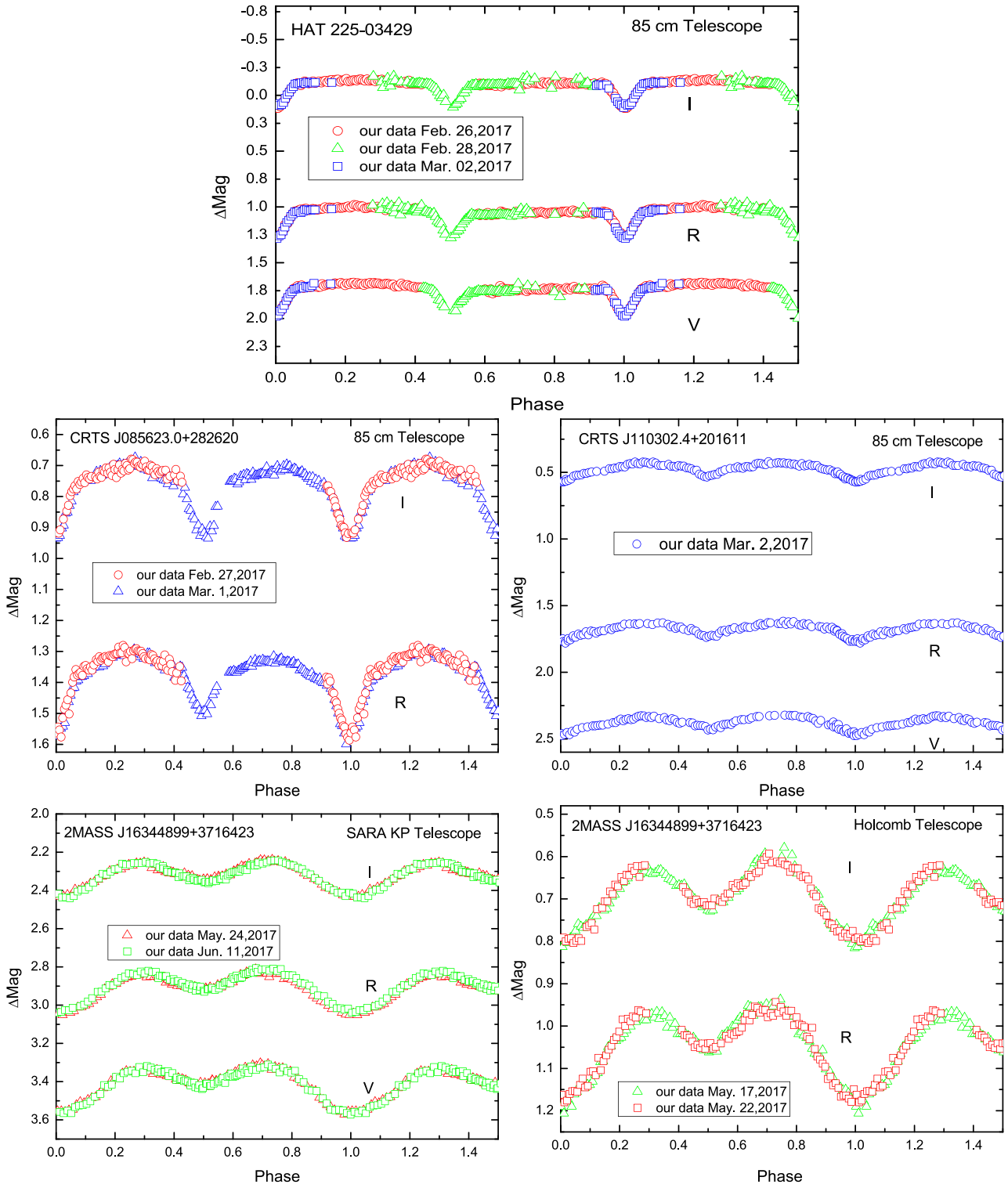

Figure 1. *V*, *R*, and *I* light curves of the four short period eclipsing binaries. Different symbols represent data observed at the different times. The vertical axis is the magnitude differences between our objects and comparison stars.

0.57 for 2MASS J16344899+3716423, respectively. For HAT 225-03429, we simultaneously analyzed our light curves and the radial velocities published by Lee & Lin (2017) to find the mass ratio $q = 0.79$ and other orbital parameters. The adjustable parameters for mode 2 are the orbital inclination i, the secondary components temperature T_2, the dimensionless potentials of the two components Ω_1 and Ω_2, and the monochromatic luminosity of the primary(L_{1V}, L_{1R} and L_{1I}).

Some of the theoretical light curves obtained by the WD program cannot fit well because of the existence of the O'Connell effect. We used the spot model to explain the distortion in the light curves. We assumed the latitude of

Table 3
Observational Data of the Four Low-mass M-type Eclipsing Binaries Obtained in 2017

Star Name	HJD_V	ΔMag _V	HJD_R	ΔMag _R	HJD_I	ΔMag_I
HAT-225-03249	2457810.9875	1.744	2457810.9817	1.057	2457810.9822	−0.101
HAT-225-03249	2457810.9899	1.737	2457810.9827	1.067	2457810.9831	−0.108
…	…	…	…	…	…	…
HAT-225-03249	2457811.3368	1.719	2457811.3302	1.009	2457811.3281	−0.106
HAT-225-03249	2457811.3393	1.720	2457811.3328	1.023	2457811.3307	−0.106
…	…	…	…	…	…	…
HAT-225-03249	2457813.0470	1.724	2457812.9847	0.984	2457812.9855	−0.170
HAT-225-03249	2457813.0493	1.724	2457812.9948	1.023	2457812.9957	−0.122
…	…	…	…	…	…	…
HAT-225-03249	2457814.9633	1.751	2457814.9643	1.041	2457815.0481	−0.087
HAT-225-03249	2457814.9657	1.737	2457814.9666	1.052	2457815.0504	−0.097
…	…	…	…	…	…	…
HAT-225-03249	2457815.0451	1.683	2457815.0461	1.025		
HAT-225-03249	2457815.0655	1.689	2457815.0666	1.019		
CRTS J085623.0+282620			2457812.0482	1.383	2457812.0487	0.766
CRTS J085623.0+282620			2457812.0497	1.405	2457812.0504	0.765
…	…	…	…	…	…	…
CRTS J085623.0+282620			2457814.0602	1.368	2457814.0611	0.752
CRTS J085623.0+282620			2457814.0622	1.365	2457814.0631	0.749
CRTS J110302.4+201611	2457815.1739	2.373	2457815.1749	1.692	2457815.1754	0.501
CRTS J110302.4+201611	2457815.1764	2.393	2457815.1774	1.684	2457815.1779	0.510
…	…	…	…	…	…	…
CRTS J110302.4+201611	2457815.4906	2.420	2457815.4941	1.726	2457815.4921	0.575
CRTS J110302.4+201611	2457815.4931	2.556				
2MASS J16344899+3716423			2457890.5779	0.949	2457890.5803	0.674
2MASS J16344899+3716423			2457890.5795	0.954	2457890.5823	0.659
…	…	…	…	…	…	…
2MASS J16344899+3716423			2457895.6843	0.988	2457895.6854	0.657
2MASS J16344899+3716423			2457895.6865	1.000	2457895.6876	0.668
…	…	…	…	…	…	…
2MASS J16344899+3716423	2457897.6411	3.345	2457897.6422	2.844	2457897.6431	2.294
2MASS J16344899+3716423	2457897.6443	3.329	2457897.6454	2.856	2457897.6463	2.290
…	…	…	…	…	…	…
2MASS J16344899+3716423	2457915.6520	3.349	2457915.6526	2.858	2457915.6535	2.279
2MASS J16344899+3716423	2457915.6547	3.351	2457915.6558	2.848	2457915.6567	2.285
…	…	…	…	…	…	…
2MASS J16344899+3716423	2457915.9768	3.320	2457915.9811	2.806	2457915.9789	2.263
2MASS J16344899+3716423	2457915.9800	3.283			2457915.9821	2.268

(This table is available in its entirety in machine-readable form.)

the spot to be 90°, which means the spots are located on the equator of the components. Next, we needed to adjust the other three parameters (longitude, radius, and temperature) of each spot separately until convergence or the sum of squares of residuals reach minimum values. The specific steps to obtain the orbital parameters are similar to those used in previous work (Zhang et al. 2014). In Tables 5 and 6, we listed the corresponding orbital parameters and spot parameters of these four eclipsing binaries. The observed and theoretical light curves for these four systems are plotted in Figure 4, and corresponding geometric structures at phases 0.25 and 0.75 as shown in Figure 5. For HAT 225-03429, we plotted the observed radial velocities from Lee & Lin (2017) using one of the primary minima (2457811.1609) and our theoretical fit using the WD program as shown in Figure 6. Lee & Lin (2017) obtained radial velocity measurements at phase ∼0.25, but the phase we obtained was ∼1. The reason may be that the initial moment is different.

4.2. The Chromospheric Activity Analysis

It is common to use these spectra lines (H_α, H_β, H_γ, H_δ, and Ca II H&K) as a way of diagnosing whether late-type stars have chromospheric activities. In optical bands, the chromospheric activity of M stars shows the emissions above continuum or core emissions in these lines. The equivalent width of the spectral line (EWs) is calculated based on the formula

$$\mathrm{EW} = \int_{\mathrm{line}} \frac{F_\lambda - F_c}{F_c}\, d\lambda \qquad (6)$$

where F_λ is the line flux and F_c is that at the continuum. The line regions (8 Å wide centered on the lines) and the spectral regions for assessing the continuum at the two sides of each line are listed in Table 8. We used the Hammer program to measure the chromospheric EWs of the H_α and the other lines (Hawley et al. 2002; West et al. 2004a; Covey et al. 2007, 2014); it computes EWs based on Equation (6). The EWs of the

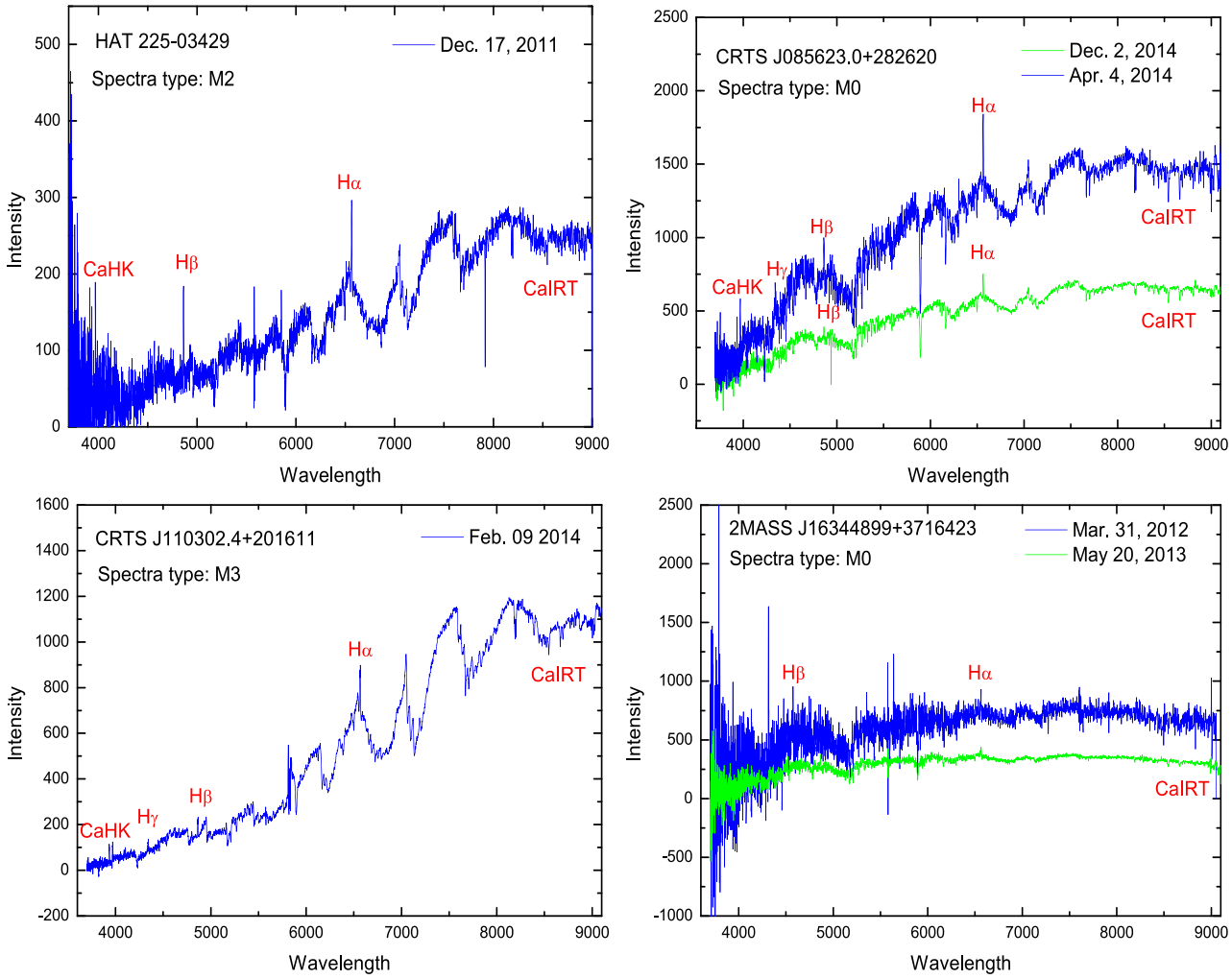

Figure 2. Low-dispersion spectra of the four low-mass M-type eclipsing binaries observed by LAMOST.

Table 4
New Minimum Times of the Four Low-mass M-type Eclipsing Binaries

Star Name	*V*		*R*		*I*		Mean (*VRI*)		Min
	HJD 245,+	Error	HJD 245,+	Error	HJD 245,+	Error	HJD 245,+	Error	1/2
	7811.1607	0.0001	7811.1609	0.0001	7811.1610	0.0001	7811.1609	0.0001	1
HAT 225-03429	7813.0803	0.0008	7813.0808	0.0002	7813.0819	0.0001	7813.0810	0.0004	2
	7815.0819	0.0001	7815.0819	0.0001	7815.0829	0.0001	7815.0824	0.0001	1
	…	…	7812.0757	0.0001	7812.0750	0.0002	7812.0754	0.0002	1
CRTS J085623.0+282620	…	…	7814.2053	0.0002	7814.2058	0.0001	7814.2055	0.0001	1
	…	…	7814.3830	0.0003	7814.3848	0.0009	7814.3839	0.0006	2
CRTS J110302.4+201611	7815.1974	0.0002	7815.1973	0.0003	7815.1957	0.0002	7815.1968	0.0002	1
	7815.3393	0.0004	7815.3422	0.0005	7815.3395	0.0003	7815.3403	0.0004	2
	7897.6792	0.0010	7897.6795	0.0008	7897.6846	0.0010	7897.6811	0.0009	2
	7897.8066	0.0005	7897.8072	0.0005	7897.8061	0.0003	7897.8066	0.0004	1
	7897.9252	0.0007	7897.9242	0.0005	7897.9269	0.0002	7897.9254	0.0004	2
	7915.6910	0.0011	7915.6907	0.0004	7915.6920	0.0007	7915.6912	0.0007	2
2MASS J16344899+3716423	7915.8159	0.0005	7915.8174	0.0003	7915.8172	0.0004	7915.8168	0.0004	1
	7915.9356	0.0012	7915.9365	0.0014	7915.9380	0.0009	7915.9367	0.0012	2
	…	…	7890.6517	0.0005	7890.6531	0.0007	7890.6524	0.0006	1
	…	…	7890.7692	0.0008	7890.7722	0.0006	7890.7707	0.0007	2
	…	…	7895.7071	0.0004	7895.7060	0.0005	7895.7065	0.0005	2
	…	…	7895.8324	0.0005	7895.8332	0.0003	7895.8328	0.0004	1

Note. A value of 1 represents the primary minimum, and 2 represents the secondary one.

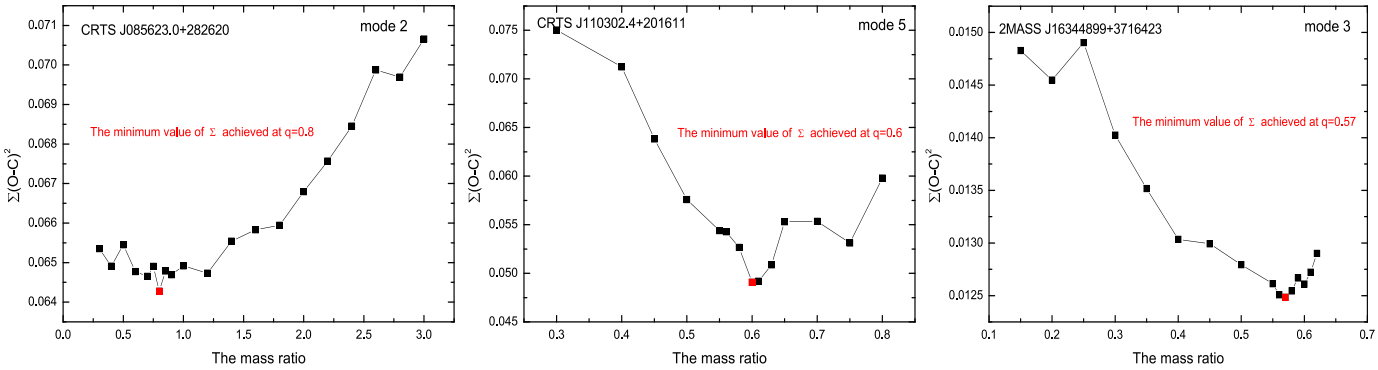

Figure 3. Relation between the sum of the squares of the residuals and the mass ratio q for CRTS J085623.0+282620, CRTS J110302.4+201611, and 2MASS J16344899+3716423.

Table 5
Orbital Parameters for the Four Low-mass M-type Eclipsing Binaries

Element	HAT 225-03429	CRTS J085623.0+282620	CRTS J110302.4+201611	2MASS J16344899+3716423
Mode	2	2	5	3
T_1	4400Ka	4173Ka	4374Ka	4466Ka
q	0.79 ± 0.1	0.8 ± 0.1	0.6 ± 0.1	0.57 ± 0.1
i	80.634 ± 0.003	69.525 ± 0.015	65.746 ± 0.010	32.790 ± 0.229
T_2	4312 ± 13K	4025 ± 7K	2960 ± 11K	3733 ± 38K
Ω_1	4.5542 ± 0.0066	4.7927 ± 0.0589	7.3189 ± 0.0279	2.5909 ± 0.0018
Ω_2	7.4623 ± 0.0573	3.6269 ± 0.0088	3.0634a	2.5909a
$L_{1V}/(L_1+L_2)_V$	0.8401 ± 0.0009	…	0.8035 ± 0.0001	0.8553 ± 0.0022
$L_{1R}/(L_1+L_2)_R$	0.8374 ± 0.0008	0.4291 ± 0.0033	0.7170 ± 0.0002	0.8295 ± 0.0026
$L_{1I}/(L_1+L_2)_I$	0.8332 ± 0.0008	0.4137 ± 0.0039	0.5731 ± 0.0005	0.7724 ± 0.0028
r_1(pole)	0.2640 ± 0.0020	0.2489 ± 0.0037	0.1486 ± 0.0042	0.4813 ± 0.0033
r_1(point)	0.2772 ± 0.0026	0.2590 ± 0.0044	0.1495 ± 0.0043	…
r_1(side)	0.2686 ± 0.0022	0.2525 ± 0.0039	0.1490 ± 0.0042	0.5369 ± 0.0053
r_1(back)	0.2742 ± 0.0024	0.2569 ± 0.0042	0.1494 ± 0.0043	0.6451 ± 0.0148
r_2(pole)	0.1247 ± 0.0017	0.3110 ± 0.0013	0.3142 ± 0.0009	0.3942 ± 0.0038
r_2(point)	0.1254 ± 0.0017	0.3636 ± 0.0029	0.4476 ± 0.0011	0.4349 ± 0.0057
r_2(side)	0.1249 ± 0.0017	0.3223 ± 0.0015	0.3283 ± 0.0020	…
r_2(back)	0.1254 ± 0.0017	0.3428 ± 0.0020	0.3606 ± 0.0015	…
a($R_\odot$)	2.134 ± 0.320	2.051 ± 0.246	1.496 ± 0.264	1.538 ± 0.181
$M_1(M_\odot)$	0.40 ± 0.06	0.51 ± 0.06	0.34 ± 0.06	0.51 ± 0.06
$M_2(M_\odot)$	0.32 ± 0.05	0.41 ± 0.05	0.20 ± 0.04	0.29 ± 0.03
$R_1(R_\odot)$	0.58 ± 0.08	0.52 ± 0.06	0.22 ± 0.04	0.85 ± 0.05
$R_2(R_\odot)$	0.27 ± 0.04	0.69 ± 0.08	0.54 ± 0.09	0.64 ± 0.07
$\sum(O-C)_i^2$	0.1013	0.0508	0.0389	0.0078

Note. Parameters not adjusted in the solution are denoted by "a."

Table 6
Spot Parameters of the Four Low-mass M-type Eclipsing Binaries

Star	HJD(245,+)	Spot Location	Colatitude	Longitude	Radius	T(s)
HAT 225-03429	7813.0	P	90° a	254.°0 ± 0.°2	12.°7 ± 0.°5	3664 K ± 29 K
CRTS J085623.0+282620	7812.0	P	90° a	264.°2 ± 1.°2	12.°7 ± 0.°3	3218 K ± 142 K
CRTS J110302.4+201611	7815.1	P	90° a	50.°1 ± 0.°6	11.°3 ± 0.°9	3348 K ± 203 K
2MASS J16344899+3716423	7890.5	P	90° a	212.°0 ± 0.°9	14.°1 ± 1.°2	5291 ± 50 K
2MASS J16344899+3716423	7897.7	P	90° a	215.°5 ± 0.°5	12.°3 ± 0.°5	5565 K ± 38 K
2MASS J16344899+3716423	7915.8	P	90° a	221.°9 ± 1.°2	11.°5 ± 0.°3	5615 K ± 62 K

spectral lines confirm the chromospheric activities of these four low-mass M-type eclipsing binaries, and the results are listed in Table 7, including the star name, observation time, spectral type, and EWs of the H_α, H_β, H_γ, H_δ, and Ca II H&K lines.

5. Discussions and Conclusions

5.1. Orbital Parameters

Through our photometric observations and analyses, we obtained new light minima times and updated linear ephemerides

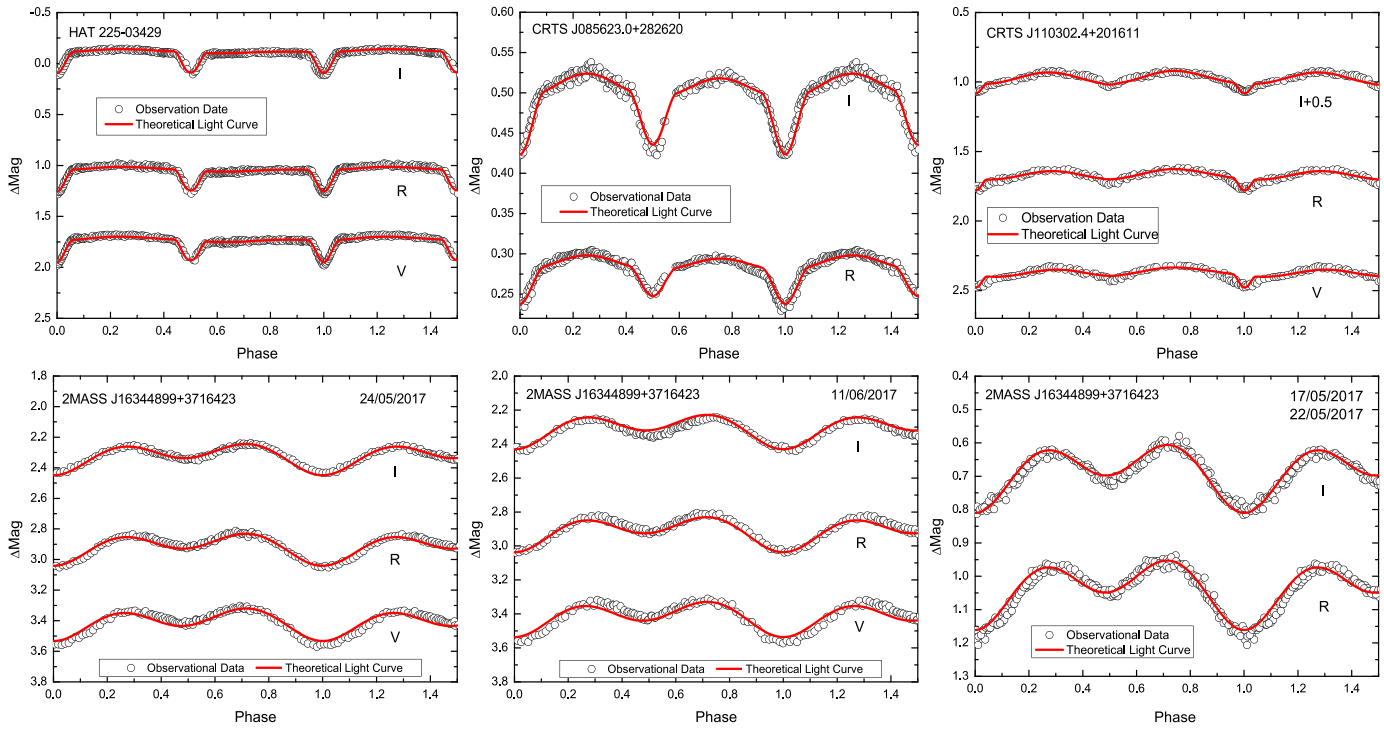

Figure 4. Observational and theoretical light curves of the four low-mass M-type eclipsing binaries. The points and solid lines represent the observational and theoretical light curves, respectively.

for four low-mass M-type eclipsing binaries. For three of these four binary systems (CRTS J085623.0+282620, CRTS J110302.4+201611, and 2MASS J16344899+3716423), this is the first time that their orbital parameters have been obtained using the Wilson–Devinney program. The asymmetric light curves of these four low-mass M-type eclipsing binaries indicate that there are starspot activities on the component stars of these binary systems.

The light curves of HAT 225-03429 show that it is a detached eclipsing binary. In analyzing the orbital parameters for HAT 225-03429, we included our new light curves and the radial velocities published by Lee & Lin (2017). The spectroscopic mass ratio is 0.79, which is larger than the previous result (0.72) derived by Lee & Lin (2017). The orbital inclination is 80°.9 (±0.01), which is also larger than their value of 73°.5 (±0.02) (Lee & Lin 2017). This may be because we used the detached mode (mode 2) of the WD program, the mass ratio is ill-constrained from light curves alone (Wyithe & Wilson 2002), and we considered the starspot effect. Based on information from the Catalina Sky Survey, we first used mode 3 to analyze the orbital physics of CRTS J085623.0+282620 and CRTS J110302.4+201611. However, the resulting dimensionless potentials are larger than the Ω_{in}. After trying several configurations, we conclude that CRTS J085623.0+282620 is a detached eclipsing binary and CRTS J110302.4+201611 is a semi-detached eclipsing binary; these results are different from those obtained by Drake et al. (2014). The orbital inclinations of CRTS J085623.0+282620 and CRTS J110302.4+201611 are 69°.5 (±0.02) and 65°.7 (±0.01), respectively. The photometric solution indicates that 2MASS J16344899+3716423 is a contact binary ($i = 32°.8$ (±0.2), $q = 0.57$). The asymmetry of the light curves indicates that these four systems have starspot activities. For 2MASS J16344899+3716423, we found three complete sets of light curves and obtained starspot parameters corresponding to three different observation times. The longitudes of the starspots did not change significantly.

Based on our light curves and spectral analysis, we obtained the spectral types and orbital parameters. Using the Cox relation (Cox 2000), we estimated the masses of primary stars based on the spectral types. We then combined the mass ratio (see Table 5) to calculate the masses of secondary stars. Utilizing Kepler's third law ($M_1 + M_2 = 0.0134a^3/p^2$), we calculated the semimajor axis a of our objects. The radii of each components could be derived using formula $R_{1,2} = a \times r_{1,2(\mathrm{mean})}$, where $r_{1,2(\mathrm{mean})}$ is the mean fractional radii of each component in the photometric solutions (see Table 5). We used the error transfer formula to determine their errors. The absolute parameters and errors are listed in Table 5. In Figure 7, we plotted the radius–mass relationship with a mass range of 0.1–1.2 $M_\odot$. The mass tracks and isochrones were adopted from Baraffe et al. (1998) and Bayless & Orosz (2006). The dashed lines represent the isochrones of Baraffe et al. (1998) models with log ages (years) = 7.0, 7.1, 7.2, and 7.8, respectively, and the solid line represents an empirical mass–radius relationship of the formula $R(R_\odot) = 0.0324 + 0.9343M(M_\odot) + 0.0374M^2(M_\odot)$ by Bayless & Orosz (2006). Compared to this relationship, the secondary component of HAT 225-03429 and the primary component of CRTS J085623.0+282620 agree quite well, whereas the other component stars are located somewhat far from the solid line. The primary components of HAT 225-03429, 2MASS J16344899+3716423, and the secondary components of CRTS J085623.0+282620, CRTS J110302.4+201611, and 2MASS J16344899+3716423 appear to be quite evolved with over-radius. Ribas (2006) proposed the possibility that high-level stellar activity would result in the radii of low-mass eclipsing binaries being larger than what is predicted. Our photometric and spectroscopic analyses indicate that these four systems are active. However, it is still uncertain whether larger

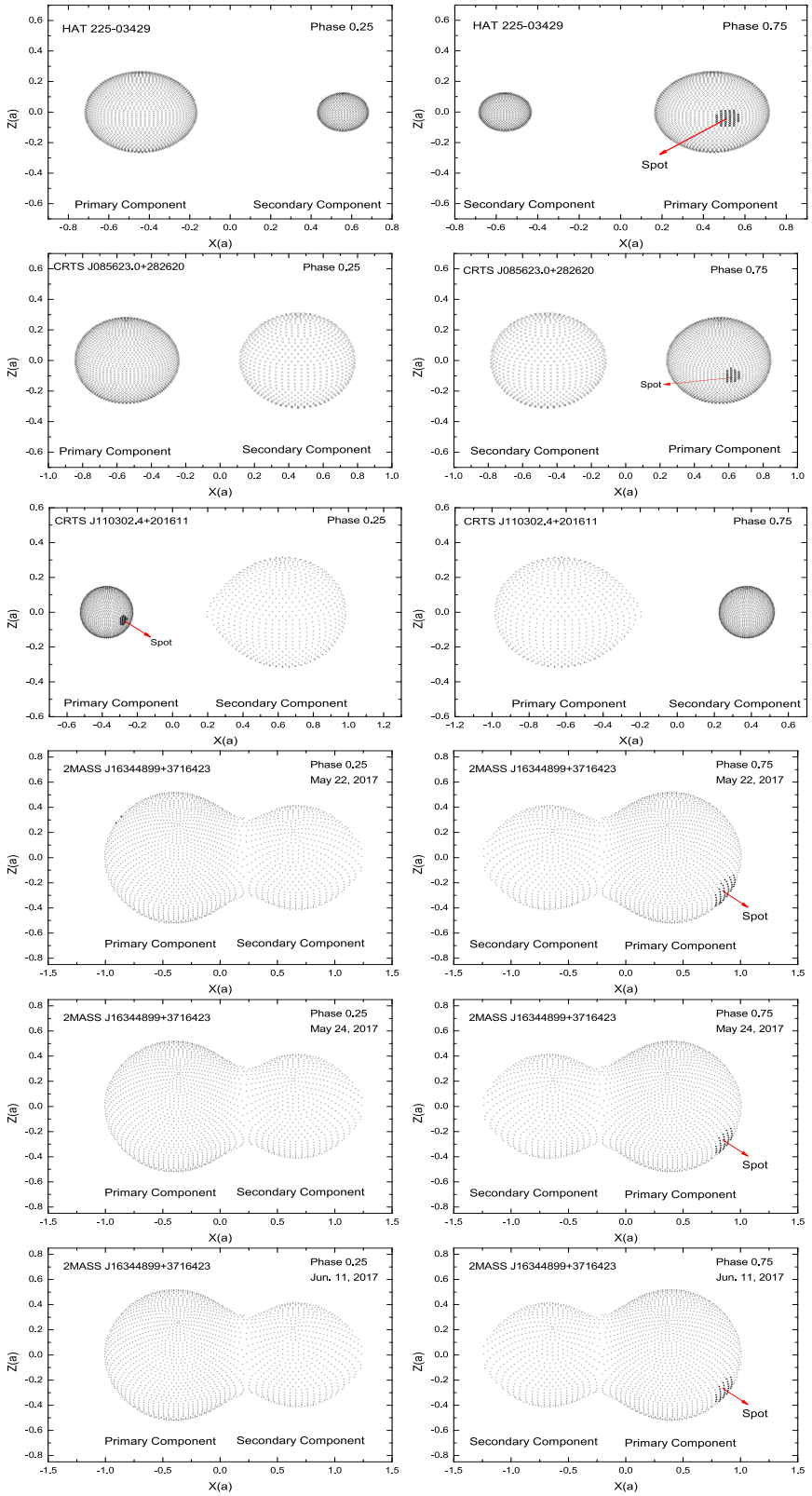

Figure 5. The star and starspot configurations of the four low-mass eclipsing binaries. The unit (a) is the orbital separation between the mass centers of the two components.

radii are really caused by magnetic activity. As shown in Figure 7, two component stars of 2MASS J16344899+3716423 and the secondary star of CRTS J110302.4+201611 are near the log ages (years) = 7.1 isochrone, indicating that the ages of their are about 126 Myr. The primary star of HAT 225-03429 is located between log ages (years) = 7.2 and 7.8 isochrones, suggesting that its age is about 158 ∼ 631 Myr. For the secondary star of CRTS J085623.0+282620, we estimated its

Table 7
EWs of Chromospheric Active Lines for the Four Low-mass M-type Eclipsing Binaries

Element	CRTS J085623.0+282620		CRTS J110302.4+201611	2MASS J16344899+3716423		HAT 225-03429
Obs-Date	2014 Dec 2nd	2014 Apr 4th	2014 Feb 9th	2013 May 20th	2012 Mar 31st	2011 Dec 17th
HJD(245,+)	6993.5029	6751.5023	6697.5053	6432.5030	6382.5020	5912.5037
Spectral type	M0	M0	M3	M0	M0	M2
H_α	1.8 ± 0.4	2.1 ± 0.1	2.7 ± 0.3	1.7 ± 0.6	1.0 ± 0.3	3.8 ± 1.3
H_β	1.2 ± 0.1	1.6 ± 0.1	2.9 ± 0.1	1.3 ± 0.1	0.3 ± 0.1	5.8 ± 1.0
H_γ	1.3 ± 0.2	1.8 ± 0.2	3.9 ± 0.4	1.1 ± 0.3	−1.04 ± 0.6	8.1 ± 3.7
H_δ	0.4 ± 0.1	0.6 ± 0.1	2.6 ± 0.4	0.3 ± 0.1	4.1 ± 2.9	3.3 ± 3.1
Ca II H	1.0 ± 0.2	4.4 ± 1.9	7.2 ± 1.3	10.5 ± 11.5	−10.8 ± 17.6	14.2 ± 23.4

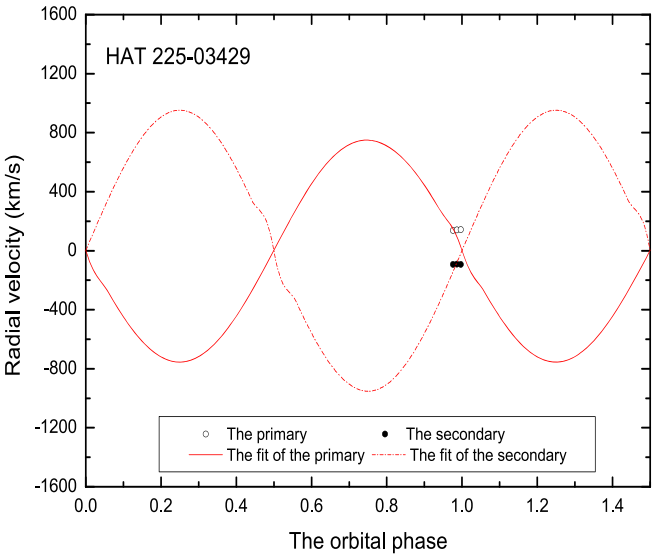

Figure 6. Radial velocities of the primary and secondary stars and their fits for HAT 225-03429.

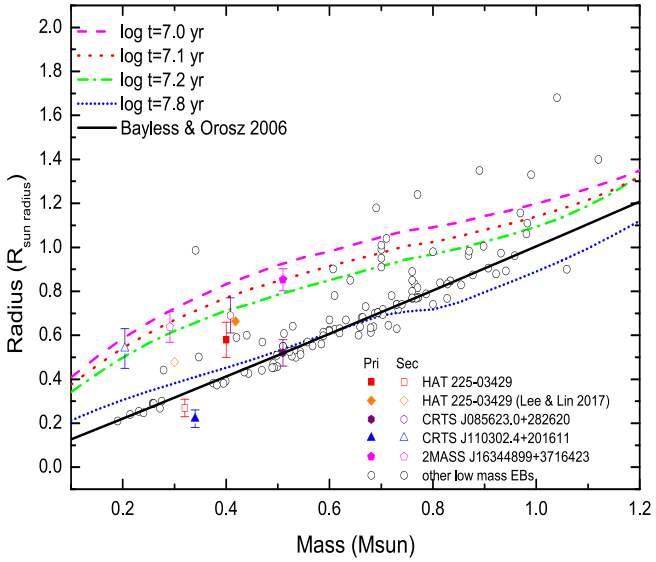

Figure 7. The mass–radius diagram of the four eclipsing binaries compared with 119 components of low-mass eclipsing binaries. The solid line is the empirical mass–radius relation derived by Bayless & Orosz (2006) and the dashed lines are the isochrones with log ages (years) = 7.0, 7.1, 7.2, and 7.8, respectively, from the stellar model of Baraffe et al. (1998).

age is 158 Myr due to it being positioned near the log ages (years) = 7.1 isochrone. The primary star of CRTS J110302.4 +201611 is located below the log age (years) = 7.8 isochrone. In order to see how the component stars from these four binaries compare with other low-mass stars, we collected orbital parameters and their standard deviations for other low-mass stars and listed them in Table 8. The mass–radius relationship of the stars in these four systems are similar to other low-mass double-lined eclipsing binaries, as shown in Figure 7. We have revised the mass and radius of both components of HAT 225-03429. For the primary component of HAT 225-03429, we revised the mass from $M_1 = 0.418\,M_\odot$ to $M_1 = 0.40\,M_\odot$ and the radius from $R_1 = 0.663\,R_\odot$ to $R_1 = 0.58\,R_\odot$. For the secondary component of HAT 225-03429, we revised the mass from $M_2 = 0.300\,M_\odot$ to $M_2 = 0.32\,M_\odot$ and the radius from $R_2 = 0.478\,R_\odot$ to $R_2 = 0.27\,R_\odot$. It seems that our results of HAT 225-03429 are somewhat discrepant from those of Lee & Lin (2017). These differences will require further verification because the JKTEBOP (Southworth et al. 2004) in Lee & Lin (2017) and our method of using the Wilson–Devinney program do not provide the error estimate using the Markov Chain Monte Carlo method for the eclipsing binaries (Boffin et al. 2018). Although the masses and radii of HAT 225-03429 were determined with the radial velocity, the results still need to be verified due to the lack of data. More data regarding radial velocity are needed for confirmation.

5.2. Chromospheric Activity

Chromospheric activity and starspot activity, triggered by magnetic fields and maintained by a magnetic dynamo, are the most important phenomena in M-type stars. There had been no prior research on the chromospheric activity indicators for these four low-mass M-type eclipsing binaries. In this study, we first noticed from the observed spectra of four low-mass M-type eclipsing binaries that the chromospheric activity indicators of H_α, H_β, H_γ, H_δ, and Ca II H&K lines show emissions (see Figure 2). We used the same method as Lu et al. (2018) to calculate the equivalent width of these chromospheric active lines. From Table 7, we can see that the equivalent widths of the H_α lines of the four M-type eclipsing binaries are greater than 0.75 Å, and the equivalent widths of the H_β, H_γ, H_δ, and Ca II H&K lines are greater than 1.0 Å. Comparing the criteria for determining the chromospheric activity of M-type stars derived by West et al. (2011), we can infer that these four low-mass M-type eclipsing binaries are active. Our photometric

Table 8
The Mass, Radius, and Orbital Period of Low-mass Stars in the Double-lined Eclipsing Binaries

Star Name	Mass ($M_\odot$)	Radius ($R_\odot$)	Period	References
BX Tri A	0.51 (2)	0.55 (1)	0.192	1
NSVS 01031772 A	0.5428 (27)	0.5260 (28)	0.368	2
NSVS 01031772 B	0.4982 (25)	0.5088 (30)	0.368	2
NGC2204-S892 A	0.733 (5)	0.719 (14)	0.452	3
NGC2204-S892 B	0.662 (5)	0.680 (17)	0.452	3
GU Boo A	0.6101 (64)	0.627 (16)	0.489	4, 5
GU Boo B	0.5995 (64)	0.624 (16)	0.489	4, 5
NSVS 02502726 A	0.714 (19)	0.645 (6)	0.560	6
NSVS 02502726 B	0.347 (12)	0.501 (5)	0.560	6
RT And B	0.907 (17)	0.906 (11)	0.629	4, 7
MG1-1819499 A	0.557 (1)	0.569 (25)	0.630	8
MG1-1819499 B	0.535 (1)	0.500 (17)	0.630	8
…	…	…	…	…
UNSW-TR 2 A	0.5290 (35)	0.6410 (5)	2.144	26
UNSW-TR 2 B	0.5120 (35)	0.6080 (6)	2.144	26
NSVS 06507557 A	0.6560 (86)	0.6000 (3)	0.520	27
NSVS 06507557 B	0.2790 (45)	0.4420 (24)	0.520	27
T-Lyr1-17236 A	0.6795 (1)	0.6340 (43)	8.430	28
T-Lyr1-17236 B	0.5226 (61)	0.5250 (52)	8.430	28
2MASS J01542930 +0053266 A	0.6590 (31)	0.6390 (83)	2.639	29
2MASS J01542930 +0053266 B	0.6190 (28)	0.6100 (93)	2.639	29
SDSS-MEB-1 A	0.2720 (2)	0.2680 (9)	0.410	30
SDSS-MEB-1 B	0.2400 (22)	0.2480 (8)	0.410	30
BD -22 5866 A	0.5881 (29)	0.6140 (45)	2.211	31
BD -22 5866 B	0.5881 (29)	0.5980 (45)	2.211	31
NSVS 11868841 A	0.8700 (74)	0.9830 (3)	0.602	27
NSVS 11868841 B	0.6070 (53)	0.9010 (26)	0.602	27
2MASS J04463285 +1901432 A	0.4700 (5)	0.5700 (2)	0.630	32
…	…	…	…	…
NSVS 5789962 A	1.04 (18)	1.68 (08)	1.456326	36
NSVS 5789962 B	0.89 (16)	1.35 (08)	1.456326	36
NSVS 3243815 A	0.76 (04)	0.77 (03)	0.864084	36
NSVS 3243815 B	0.76 (06)	0.85 (04)	0.864084	36
NSVS 6127971 A	0.80 (12)	0.74 (12)	0.541732	36
NSVS 6127971 B	0.74 (12)	0.74 (12)	0.541732	36
NSVS 3630887 A	0.64 (06)	0.85 (04)	0.460195	36
NSVS 3630887 A	0.60 (07)	0.67 (03)	0.460195	36

References. (1) Çakirli et al. (2013), (2) López-Morales et al. (2006), (3) Rozyczka et al. (2009), (4) Torres et al. (2010), (5) López-Morales & Ribas (2005), (6) Çakirli et al. (2009), (7) Popper (1994), (8) Kraus et al. (2011), (9) Irwin et al. (2009), (10) Torres & Ribas (2002), (11) Popper (1997), (12) Rozyczka et al. (2013), (13) Morales et al. (2009b), (14) Morales et al. (2009a), (15) López-Morales & Shaw (2007), (16) Feiden & Chaboyer (2012), (17) Popper et al. (1986), (18) Torres et al. (2006), (19) Bayless & Orosz (2006), (20) Ribas (2003), (21) Hartman et al. (2011), (22) Lacy et al. (2005), (23) Bass et al. (2012), (24) Irwin et al. (2011), (25) Creevey et al. (2005), (26) Young et al. (2006), (27) Çakirli et al. (2010), (28) Devor et al. (2008), (29) Becker et al. (2008), (30) Blake et al. (2008), (31) Shkolnik et al. (2008), (32) Hebb et al. (2006), (33) Dimitrov & Kjurkchieva (2010), (34) López-Morales (2007), (35) Hełminiak et al. (2011), (36) Korda et al. (2017).

solutions for these four eclipsing binaries show starspots on them, confirming that these four binaries are indeed active.

This work was supported by the Joint Research Fund in Astronomy (U1631236 and U1431114) under cooperative agreement between the NSFC and CAS. The spectral data were made by the Large Sky Area Multi-Object Fiber Spectroscopic Telescope (LAMOST), which is a National Major Scientific Project built by the Chinese Academy of Sciences. We would like to thank Dr. Frank H. Levinson for his generous financial support, which enabled Butler University to join the SARA consortium and upgrade the Holcomb telescope. The authors would also like to thank Mr. Libo Zhao from Guizhou University for helping us with grammar.

References

Baraffe, I., Chabrier, G., Allard, F., & Hauschildt, P. H. 1998, A&A, 337, 403
Bass, G., Orosz, J. A., Welsh, W. F., et al. 2012, ApJ, 761, 157
Bayless, A. J., & Orosz, J. A. 2006, ApJ, 651, 1155
Becker, A. C., Agol, E., Silvestri, N. M., et al. 2008, MNRAS, 386, 416
Berdyugina, S. V. 2005, LRSP, 2, 8
Birkby, J., Nefs, B., Hodgkin, S., et al. 2012, MNRAS, 426, 1507
Blake, C. H., Torres, G., Bloom, J. S., & Gaudi, B. S. 2008, ApJ, 684, 635
Bochanski, J. J., Hawley, S. L., & West, A. A. 2011, AJ, 141, 98
Boffin, H. M. J., Jones, D., Wesson, R., et al. 2018, arXiv:1807.11709
Browning, M. K., Weber, M. A., Chabrier, G., & Massey, A. P. 2016, AJ, 818, 189
Butler, C. J., Erkan, N., Budding, E., et al. 2015, MNRAS, 446, 4205
Çakirli, Ö, Ibanoğlu, C., & Dervisoglu, A. 2010, RMxAA, 46, 363
Çakirli, Ö, Ibanoğlu, C., & Güngör, C. 2009, NewA, 14, 496
Çakirli, Ö, Ibanoğlu, C., & Sipahi, E. 2013, MNRAS, 429, 85
Chbrier, G., Gallardo, J., & Barafffe, I. 2007, A&A, 472, L17
Clark, B. M., Blake, C. H., & Knapp, G. R. 2012, ApJ, 744, 119
Collier Cameron, A., Wilson, D. M., West, R. G., et al. 2007, MNRAS, 380, 1230
Coughlin, J. L., López-Morales, M., Harrison, T. E., et al. 2011, AJ, 141, 78
Covey, K. R., Ivezic, Z., Schlegel, D., et al. 2007, AJ, 134, 2398
Covey, K. R., West, A. A., Bochanski, J. J., & Hawley, S. L. 2014, The Hammer: An IDL Spectral Typing Suite, Astrophysics Source Code Library, ascl:1405.003
Cox, A. N. 2002, Allen's Astrophysical Quantities (Berlin: Springer)
Creevey, O. L., Benedict, G. F., Brown, T. M., et al. 2005, ApJL, 625, L127
Cruz, P., Diaz, M., Birkby, J., et al. 2018, MNRAS, 476, 5253
Cui, X.-Q., Zhao, Y.-H., Chu, Y.-Q., et al. 2012, RAA, 12, 1197
Deshpande, R., Blake, C. H., Bender, C. F., et al. 2013, AJ, 146, 156
Devor, J., Charbonneau, D., Torres, G., et al. 2008, ApJ, 687, 1253
Dimitrov, D. P., & Kjurkchieva, D. P. 2010, MNRAS, 406, 2559
Drake, A. J., Djorgovski, S. G., Mahabal, A., et al. 2009, ApJ, 696, 870
Drake, A. J., Graham, M. J., Djorgovski, S. G., et al. 2014, ApJS, 213, 9
Epchtein, N., Deul, E., Derriere, S., et al. 1999, A&A, 349, 236
Feiden, G. A., & Chaboyer, B. 2012, ApJ, 757, 42
Hartman, J. D., Bakos, G. A., Noyes, R. W., et al. 2011, AJ, 141, 166
Hawley, S. L., Covey, K. R., Knapp, G. R., et al. 2002, AJ, 123, 3409
Hebb, L., Wyse, R. F. G., Gilmore, G., & Holtzman, J. 2006, AJ, 131, 555
Hełminiak, K. G., Konacki, M., & Złoczewski, K. 2011, A&A, 527, A14
Irwin, J., Buchhave, L., Berta, Z. K., et al. 2010, ApJ, 718, 1353
Irwin, J., Charbonneau, D., Berta, Z. K., et al. 2009, ApJ, 701, 1436
Irwin, J., Quinn, S. N., Berta, Z. K., et al. 2011, ApJ, 742, 123
Kado-Fong, E., Williams, P. K. G., Mann, A. W., et al. 2016, ApJ, 833, 281
Keel, W. C., Oswalt, T., Mack, P., et al. 2017, PASP, 129, 5002
Kirkpatrick, J. D., Gelino, C. R., Cushing, M. C., et al. 2012, ApJ, 753, 156
Korda, D., Zasche, P., Wolfe, M., et al. 2017, AJ, 154, 30
Kraus, A. L., Tucker, R. A., Thompson, M. I., Craine, E. R., & Hillenband, L. A. 2011, ApJ, 728, 48
Kroupa, P., Weidner, C., Pflamm-Altenburg, J., et al. 2013, in Planets, Stars and Stellar Systems Vol. 5, ed. T. D. Oswalt & G. Gilmore (Dordrecht: Springer), 115
Kwee, K. K., & van Woerden, H. 1965, BAN, 12, 327
Lacy, C. H. S., Torres, G., Claret, A., & Vaz, L. P. R. 2005, AJ, 130, 2838
Law, N. M., Kulkarni, S. R., Dekany, R. G., et al. 2009, PASP, 121, 1395
Lee, C.-H., & Lin, C.-C. 2017, RAA, 17, 15
López-Morales, M. 2007, ApJ, 660, 732
López-Morales, M., Orosz, J. A., Shaw, J. S., et al. 2006, arXiv:astro-ph/0610225
López-Morales, M., & Ribas, I. 2005, ApJ, 631, 1120
López-Morales, M., & Shaw, J. S. 2007, in ASP Conf. Ser. 362, The Seventh Pacific Rim Conf. Stellar Astrophysics, ed. Y. W. Kang et al. (San Francisco, CA: ASP), 26
Lu, H., Zhang, L., Han, X. L., & Shi, J. 2018, Ap&SS, 363, 104
Lubin, J. B., Rodriguez, J. E., Zhou, G., et al. 2017, ApJ, 844, 134
Lucy, L. 1967, ZA, 65, 89
Luo, A.-L., Zhang, H.-T., Zhao, Y.-H., et al. 2012, RAA, 12, 1243

Luo, A.-L., Zhao, Y.-H., Zhao, G., et al. 2015, RAA, 15, 1095
Martín, E. L., Guenther, E., Barrado y Navascués, D., et al. 2005, AN, 326, 1015
Morales, J. C., Gallardo, J., Ribas, I., et al. 2010, ApJ, 718, 502M
Morales, J. C., Ribas, I., Jordi, C., et al. 2009a, ApJ, 691, 1400
Morales, J. C., Torres, G., Marschall, L. A., & Brehm, W. 2009b, ApJ, 707, 671
Nefs, S. V., Birkby, J. L., Snellen, I. A. G., et al. 2012, MNRAS, 425, 950
Nefs, S. V., Birkby, J. L., Snellen, I. A. G., et al. 2013, MNRAS, 431, 3240
Nelson, R. H. 2007, Software by Bob Nelson, https://www.variablestarssouth.org/software-by-bob-nelson/
Nutzman, ., & Charbonneau, D. 2008, PASP, 120, 317
Pineda, J. S., West, A. A., Bochanski, J. J., & Burgasser, A. J. 2013, AJ, 146, 50
Plibulla, T., Chochol, D., & Vittone, A. A. 2003, ChJAA, 3, 361
Popper, D. M. 1994, AJ, 108, 1091
Popper, D. M. 1997, AJ, 114, 1195
Popper, D. M., Lacy, C. H., Frueh, M. L., & Turner, A. E. 1986, AJ, 91, 383
Rajpurohit, A. S., Allard, F., Teixeira, G. D. C., et al. 2018, A&A, 610, A19
Rau, A., Kulkarni, S. R., Law, N. M., et al. 2009, PASP, 121, 1334
Raymond, S. N., Szkody, P., Hawley, S. L., et al. 2003, AJ, 125, 2621
Ribas, I. 2003, A&A, 398, 239
Ribas, I. 2006, AP&SS, 304, 89R
Rozyczka, M., Kaluzny, J., Pietrukowicz, P., et al. 2009, AcA, 59, 385
Rozyczka, M., Pietrukowicz, P., Kaluzny, J., et al. 2013, MNRAS, 429, 1840
Rucinski, S. M. 1969, AcA, 19, 245
Shkolnik, E., Liu, M. C., Reid, I. N., et al. 2008, ApJ, 682, 1248
Skrutskie, M. F., Cutri, R. M., Stiening, R., et al. 2006, AJ, 131, 1163
Southworth, J., Maxted, P. F. L., & Smalley, B. 2004, MNRAS, 351, 1277
Strassmeier, D. 2009, A&ARv, 17, 251
Torres, G., Andersen, J., & Giménez, A. 2010, A&ARv, 18, 67
Torres, G., Lacy, C. H., Marschall, L. A., Sheets, H. A., & Mader, J. A. 2006, ApJ, 640, 1018
Torres, G., & Ribas, I. 2002, ApJ, 567, 1140
Van Hamme, W. 1993, AJ, 106, 2096
West, A. A., Hawley, S. L., Walkowicz, L. M., et al. 2004a, AJ, 128, 426
West, A. A., Hawley, S. L., & Walkowicz, L. M. 2004b, AJ, 128, 426
West, A. A., Morgan, D. P., Bochanski, J. J., et al. 2011, AJ, 141, 97
West, A. A., Weisenburger, K. L., Irwin, J., et al. 2015, ApJ, 812, 3
Wilson, R. E. 1990, ApJ, 356, 613
Wilson, R. E. 1994, PASP, 106, 921
Wilson, R. E., & Devinney, E. J. 1971, ApJ, 166, 605
Wilson, R. E., & Van Hamme, W. 2004, Computing Binary Star Observables (Gainesville, FL: Univ. Florida)
Wyithe, J. S. B., & Wilson, R. E. 2002, ApJ, 571, 293
Yi, Z. P., Luo, A. L., Song, Y. H., et al. 2014, AJ, 147, 33
York, D. G., Adelman, J., Anderson, J. E., Jr., et al. 2000, AJ, 120, 1579
Young, T. B., Hidas, M. G., Webb, J. K., et al. 2006, MNRAS, 370, 1529
Zhang, L. Y., Lu, H. P., Han, X. M., et al. 2018, NewA, 61, 36
Zhang, L. Y., Pi, Q. F., Han, X. M., et al. 2016, NewA, 44, 66
Zhang, L. Y., Pi, Q. F., & Yang, Y. G. 2014, MNRAS, 442, 2620
Zhang, L. Y., Yue, Q., Lu, H. P., et al. 2017, RAA, 17, 10
Zhao, G., Zhao, Y. H., Chu, Y. Q., et al. 2012, RAA, 12, 723
Zhou, A. Y., Jiang, X. J., Zhang, Y. P., et al. 2009, RAA, 9, 349